

## Intraband and interband magneto-optics of $p$ -type $\text{In}_{0.18}\text{Ga}_{0.82}\text{As}/\text{GaAs}$ quantum wells

R. J. Warburton and R. J. Nicholas

*Clarendon Laboratory, Parks Road, Oxford OX1 3PU, United Kingdom*

L. K. Howard

*Strained Layer Research Group, University of Surrey, Guildford GU2 5XH, United Kingdom*

M. T. Emeny

*Royal Signals and Radar Establishment, St. Andrews Road, Great Malvern,  
Worcestershire WR14 3PS, United Kingdom*

(Received 15 January 1991)

$p$ -type 90-Å  $\text{In}_{0.18}\text{Ga}_{0.82}\text{As}/\text{GaAs}$  quantum wells with carrier concentrations in the range  $p_s = (1.5-4.3) \times 10^{11} \text{ cm}^{-2}$  have been studied by magneto-optics. Cyclotron resonance measures the effective mass of the  $|M_J| = \frac{3}{2}$  holes as  $\approx 0.16$  for in-plane motion. The mass is light because of the strain decoupling of the “heavy-hole”  $|M_J| = \frac{3}{2}$  and “light-hole”  $|M_J| = \frac{1}{2}$  states. The effective mass has been measured as a function of carrier concentration and field. The totally decoupled limit is not achieved and the residual coupling between the  $|M_J| = \frac{3}{2}$  and  $\frac{1}{2}$  states is well described by a calculation of the Landau levels using an eight-band  $\mathbf{k}\cdot\mathbf{p}$  model. Filling-factor-related anomalies in the cyclotron resonance are observed and interpreted in terms of hole-hole interactions combined with the presence of localizing potentials. Interband photoconductivity measurements determine the conduction-band structure and good agreement with the calculations is achieved. The magnetoexciton binding energy and band filling are considered in the analysis of the interband data.

### I. INTRODUCTION

In strained quantum wells, the uniaxial component of the strain tends to decouple the “heavy-hole”  $|M_J| = \frac{3}{2}$ , and “light-hole”  $|M_J| = \frac{1}{2}$  states, leading to mass reversal effects. The  $(\text{InAl,Ga})\text{As}/(\text{Ga,Al})$  system<sup>1</sup> should be an ideal material to maximize the light-hole behavior of the  $|M_J| = \frac{3}{2}$  subbands, because for a given strain splitting, it is possible to further reduce the  $|M_J| = \frac{3}{2}$  and  $\frac{1}{2}$  coupling by spatially separating the  $|M_J| = \frac{3}{2}$  and  $|M_J| = \frac{1}{2}$  wave functions. Experimentally, this system is convenient, as high-quality samples can be produced either by molecular-beam epitaxy (MBE) or metalorganic vapor-phase epitaxy. The mass reversal effect was first observed<sup>2</sup> in temperature-dependent magnetotransport measurements on  $p$ -type  $\text{In}_x\text{Ga}_{1-x}\text{As}/\text{GaAs}$  superlattices. Since then, the  $|M_J| = \frac{3}{2}$  mass has been directly measured<sup>3,4</sup> by cyclotron resonance. Masses of  $\sim 0.15$  have been recorded. However, the  $|M_J| = \frac{3}{2}$  subband dispersion is highly nonparabolic,<sup>5,6</sup> and the nonparabolicity contribution to the effective mass depends inversely on the  $|M_J| = \frac{3}{2}$  and  $\frac{1}{2}$  splitting. Device possibilities are discussed by O’Reilly.<sup>7</sup> The strain reconstructed valence band is considerably simpler than the valence band of typical lattice-matched heterostructures,<sup>8,11</sup> and so strained samples are ideal for studies of quasi-two-dimensional holes.

Well-resolved exciton features have been commonly seen in interband optical work<sup>12-15</sup> for both  $\text{In}_x\text{Ga}_{1-x}\text{As}/\text{GaAs}$  quantum wells and superlattices.

The general conclusions are that most of the band offset appears in the conduction band, and that for moderate strains the system is type II for “light” holes. Interband magneto-optics has been used to measure the reduced effective mass, and to demonstrate how genuine superlattice band structure can be achieved with this system.<sup>15</sup>

In this paper we report the results of both intraband and interband magneto-optics of single  $p$ -type  $\text{In}_{0.18}\text{Ga}_{0.82}\text{As}/\text{GaAs}$  quantum wells. We have measured the effective masses up to 17 T for a range of carrier concentrations  $(1.5-4.3) \times 10^{11} \text{ cm}^{-2}$ . The Landau levels have been calculated with an eight-band  $\mathbf{k}\cdot\mathbf{p}$  model, and good agreement with the experimental data is achieved when the theory is interpreted in a one-particle, intrinsic way. However, various filling-factor-related anomalies are observed. These anomalies show that hole-hole interactions must be taken into account, and they also reveal the existence of localizing potentials.

### II. EXPERIMENTAL DETAILS

The samples were grown by MBE at the R.S.R.E. Laboratory in Malvern. Four samples were studied, each with indium concentration of 18% and 90-Å well width. The samples were  $p$ -type modulation doped. The carrier concentration was controlled via the widths of the doped regions on either side of the quantum well. The sample details are summarized in Table I.

The low-temperature carrier concentration ( $p_s$ ) of the two samples with the lowest doping could be significantly increased by a persistent photoconductivity effect.

TABLE I. The sample details. The low-temperature carrier concentrations are given before (dark) and after (light) illumination from above band-gap radiation.

Sample	dark $p_s$ ( $10^{11} \text{ cm}^{-2}$ )	light $p_s$ ( $10^{11} \text{ cm}^{-2}$ )
ME541	1.5	1.8
ME539	2.6	3.7
ME538	3.7	4.0
ME540	4.2	4.3

Table I shows how the samples span the carrier concentration range  $(1.5\text{--}4.3)\times 10^{11} \text{ cm}^{-2}$ . Mobilities were  $\sim 5000\text{--}15\,000 \text{ cm}^2 (\text{V s})^{-1}$ .

For the cyclotron resonance experiments, we employed a fast-scan Fourier-transform spectrometer and a superconducting magnet. Each sample was studied up to 14.5 T, but ME540 was taken to 17 T with a higher field magnet, as discussed in Sec. IV. The radiation was detected by a silicon bolometer placed directly behind the sample, both at about 3.5 K. The carrier concentrations were measured in separate low-temperature transport experiments. The interband photoresponse (to unpolarized radiation) was detected by photoconductivity. Contacts to the samples were made by alloying In-Zn ( $\sim 5\%$  Zn) into the surface at  $\sim 300^\circ\text{C}$ . A constant current passed through the sample, and the voltage from the same two contacts was used to measure the photoconduction. A four-contact measurement gave no systematic differences to the results. Interband spectra were recorded up to 15 T.

### III. LANDAU-LEVEL CALCULATIONS

We have calculated the Landau levels of a  $90\text{-}\text{\AA}$   $\text{In}_{0.18}\text{Ga}_{0.82}\text{As}/\text{GaAs}$  quantum well with an eight-band  $\mathbf{k}\cdot\mathbf{p}$  model. The basis states correspond to the conduction, heavy-hole, light-hole, and spin-orbit bands. The Hamiltonian and its origin are discussed elsewhere.<sup>16</sup> The boundary conditions adopted conserve the envelope function and envelope function “current” at the inter-

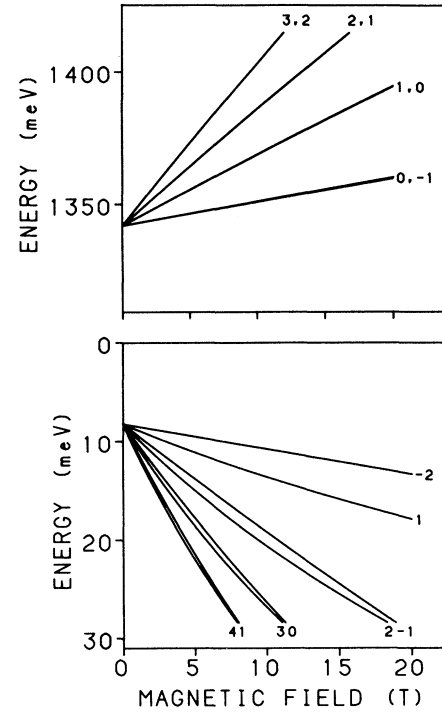


FIG. 1. The conduction-band (upper plot) and valence-band (lower plot) Landau levels for a single  $\text{In}_{0.18}\text{Ga}_{0.82}\text{As}/\text{GaAs}$  quantum well calculated with eight-band  $\mathbf{k}\cdot\mathbf{p}$  theory. The energy zero is at the top of the “heavy-hole” quantum well, and the lowest energy of the conduction-band plot is the bottom of the conduction-band well.

faces.<sup>17</sup> The conventional assumption of Bloch function equality for well and barrier materials is adopted, and is likely to be a very good one in this case when the well and barrier materials are quite similar electronically. The strain is included with the valence-band Hamiltonian of Pikus and Bir,<sup>18</sup> and a hydrostatic term is added to the two conduction-band diagonal Hamiltonian elements. We make two approximations in implementing the mod-

TABLE II. The parameters used in the Landau-level calculations for  $\text{In}_{0.18}\text{Ga}_{0.82}\text{As}/\text{GaAs}$  quantum wells.

Parameter	GaAs	$\text{In}_{0.18}\text{Ga}_{0.82}\text{As}$
Band gap (eV) $E_g(x) = 1.519 - 1.5387x + 0.475x^2$	1.519	1.257 4
Spin-orbit splitting (eV) $\Delta(x) = 0.341 - 0.09x + 0.14x^2$	0.341	0.329
Kane matrix element (eV) $E_p$	25.7	25.7
Conduction-band mass $m_c = 0.0665 - 0.0435x$	0.0665	0.058 67
Heavy-hole mass $m_{hh}^{001}$	0.34	0.34
Heavy-hole mass $m_{hh}^{111}$	0.725	0.725
Light-hole mass $m_{lh}^{001} = 0.0942 - 0.062x$	0.0942	0.083 04
Luttinger parameter $\kappa_l$	1.2	1.8
Lattice constant ( $\text{\AA}$ ) $a_0(x) = 5.65 + 0.43x$	5.65	5.727 4
Elastic constant (kbar) $C_{11}(x) = 1223 - 390x$	1223	1153
Elastic constant (kbar) $C_{12}(x) = 571 - 118x$	571	550
Deformation potential (eV) $b(x) = -1.7 - 0.1x$	-1.7	-1.718
Deformation potential (eV) $a(x) = -7.1 + 1.2x$	-7.1	-6.884

el. First, we assume flat bands, i.e., the effect of the doping on the potential profile is not included. Second, we use the axial approximation in which  $\gamma_2$  and  $\gamma_3$  are replaced by an average value [in this case by  $\frac{1}{2}(\gamma_2 + \gamma_3)$ ] in the following terms of the Hamiltonian:  $H_{23}$ ,  $H_{24}$ ,  $H_{67}$ , and  $H_{78}$ . Both approximations are extremely convenient numerically, and it is unlikely that they give rise to any misunderstandings when we interpret the experimental results. The input parameters for GaAs and  $\text{In}_{0.18}\text{Ga}_{0.82}\text{As}$  were taken to be compatible with those employed by Duggan and co-workers.<sup>14</sup> The parameters are listed in Table II. GaAs masses of Shanabrook *et al.*<sup>19</sup> were used, taken to vary with indium concentration, as listed in Table II. A heavy-hole well depth of 69.2 meV was assumed, corresponding to a band offset ratio  $Q_c = 0.67$ . No consensus exists regarding the band offsets and their dependence on indium concentration, but this value is reasonable.<sup>12,13,20</sup> For this offset, the light holes have a type-II alignment. Figure 1 shows the valence-band and conduction-band Landau levels for this system, with the Landau levels labeled in a standard notation.<sup>8,21</sup>

#### IV. CYCLOTRON RESONANCE

##### A. Effective-mass determination

Figure 2 is a plot of the cyclotron-resonance (CR) energy  $E_{\text{CR}}$  against magnetic field  $B$  for all four samples. The results for ME538 and ME540 after illumination are not shown, as they were the same for all intents and purposes as the data taken before illumination. Also, the results

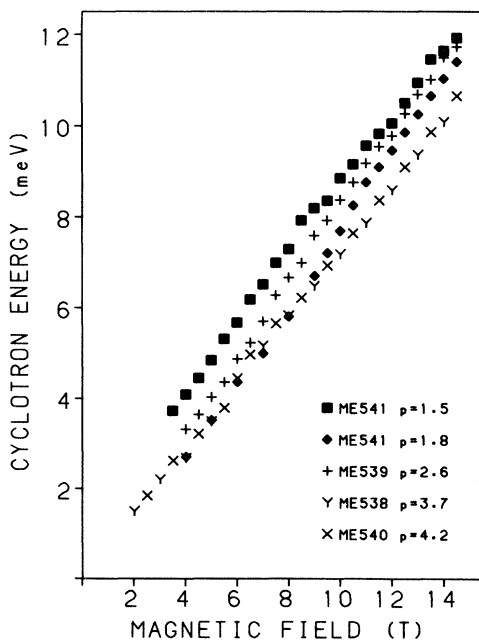


FIG. 2. The cyclotron-resonance energies plotted against magnetic field. The carrier concentrations are listed in units of  $10^{11} \text{ cm}^{-2}$ .

for ME539 after illumination ( $p_s = 3.7 \times 10^{11} \text{ cm}^{-2}$ ) are not shown, as they were very similar to the ME538 and ME540 results. A typical cyclotron resonance from ME540 ( $p_s = 4.2 \times 10^{11} \text{ cm}^{-2}$ ) is shown in the inset to Fig. 3. The cyclotron-resonance linewidth  $\Gamma_{\text{CR}}$ , quoted here as the full width at half maximum, is strongly dependent on field, varying between 0.7 and 1.4 meV for sample ME540. The corresponding optical mobilities,  $\mu_{\text{op}} = 2E_{\text{CR}} / (\Gamma_{\text{CR}} B)$ , are 10 500 and 19 000  $\text{cm}^2 (\text{V s})^{-1}$ , both of which are higher than the dc transport mobility  $\mu_{\text{dc}} \approx 7000 \text{ cm}^2 (\text{V s})^{-1}$ . Cyclotron-resonance experiments on another  $p$ -type strained-layer system,  $\text{In}_x\text{Ga}_{1-x}\text{Sb}/\text{GaSb}$  quantum wells,<sup>22</sup> also gave optical mobilities that were higher than the transport mobilities, but in this case the behavior was more extreme with  $\mu_{\text{op}}$  up to a factor of 6 higher than  $\mu_{\text{dc}}$ . Figure 2 shows that all the CR data points lie on the same curve except for those from ME541 (light and dark) and from ME539 (dark). This behavior is tied to the filling factor  $\nu$ , the number of completely filled Landau levels, where it is essential in this system to count the different spin states separately, as the spin splitting is important. We find that large deviations to the common  $E_{\text{CR}}$  versus  $B$  curve occur when  $\nu < 1$ . For instance, after illumination, ME541 has a fundamental field (the field for  $\nu = 1$ ) of 7.4

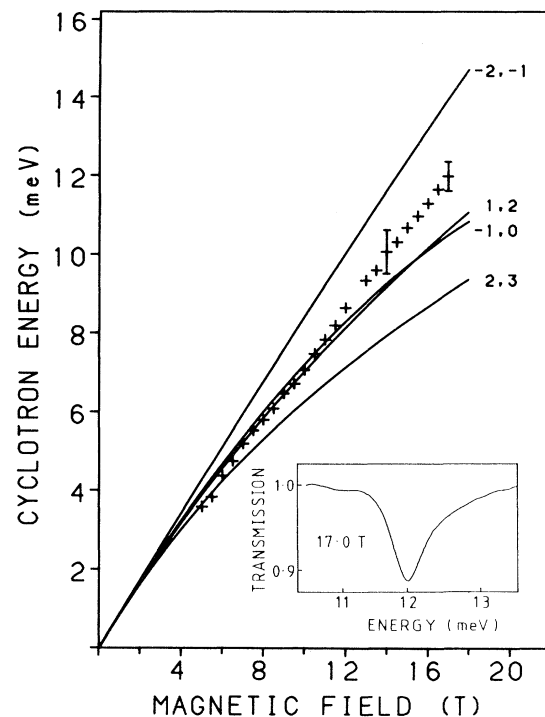


FIG. 3. Cyclotron energies plotted against magnetic field. The crosses are the data points for ME540 ( $p_s = 4.2 \times 10^{11} \text{ cm}^{-2}$ ), and the error bars represent the full width at half maximum (FWHM).  $\nu = 1$  (2) occurs at 17.4 T (8.7 T). The solid lines are the calculated energies of the  $-2 \rightarrow -1$ ,  $-1 \rightarrow 0$  (predominantly  $M_J = -\frac{3}{2}$ ), and  $1 \rightarrow 2$ ,  $2 \rightarrow 3$  (predominantly  $M_J = +\frac{3}{2}$ ) transitions.

T, and for lower fields the points line up with the others from higher hole-density resonances, whereas at higher fields in the quantum limit ( $\nu < 1$ ) the points deviate to higher energy. The reason for the enhanced  $E_{CR}$  in the quantum limit is discussed later (see Sec. IV C). Smaller anomalies in the cyclotron energy were also observed for  $\nu \sim 2$  or 3 and occurred along with a broadening of the resonance (see Sec. IV D). We point out here that the data points taken for  $\nu > 1$  and away from any linewidth anomaly can be reliably used to measure the effective mass,  $m_{CR} = e\hbar B / (m_0 E_{CR})$ , in units of the free-electron mass  $m_0$ . Within the limits imposed by these constraints, we find that the mass is 0.16, independent to within 0.005 of sample, field, and carrier concentration. The perhaps surprising absence of nonparabolicity is discussed later.

The mass is indeed low compared to the bulk GaAs heavy-hole mass of 0.34. However, the totally decoupled limit of  $(\gamma_{1l} + \gamma_{2l})^{-1} = 0.10$  is not achieved. ( $\gamma_{1l}$  and  $\gamma_{2l}$  are the conventional Luttinger parameters.<sup>23</sup>) This indicates that residual  $|M_J| = \frac{3}{2}$  and  $\frac{1}{2}$  coupling is important, which is not surprising, given that we measure cyclotron-resonance energies up to  $\approx 12$  meV, a sizable proportion of the heavy-hole–light-hole energy splitting.

To predict the cyclotron energies, the statistics of the Landau levels must be considered. The cyclotron resonance satisfies a selection rule  $\Delta n_\nu = \pm 1$ . In the quantum limit,  $\nu < 1$ , only  $n_\nu = -2$  is populated, and so only  $-2 \rightarrow -1$  is allowed. For  $1 < \nu < 2$ , holes occupy also the  $n_\nu = 1$  level, and two transitions are possible:  $-2 \rightarrow -1$  and  $1 \rightarrow 2$ , and so one would expect to see two cyclotron resonances with relative intensities determined by the statistics and overlap integrals of the respective states. At higher  $\nu$ , three transitions are always possible. An analysis along these lines has been carried out for *n*-type GaAs/Al<sub>x</sub>Ga<sub>1-x</sub>As heterojunctions.<sup>24</sup> Figure 3 shows the cyclotron-resonance data for ME540 up to 17 T. The  $-2 \rightarrow -1$  and  $1 \rightarrow 2$  calculated energies lie on either side of the data points and diverge quite rapidly at high field. The agreement between experiment and the calculation is good, provided that we assume that what we see experimentally is some sort of average of the two transitions, as only a single absorption line can be seen.

The calculations show that the valence band is highly nonparabolic. This is revealed, for instance, in Fig. 3, in which we plot the first four cyclotron-resonance transitions. The  $-1 \rightarrow 0$  and  $2 \rightarrow 3$  transitions have lower energy than their spin counterparts ( $-2 \rightarrow -1$  and  $1 \rightarrow 2$ , respectively). The nonparabolicity is larger for the  $M_J = -\frac{3}{2}$  pair ( $-2 \rightarrow -1$  and  $-1 \rightarrow 0$ ). The nonparabolicity is not revealed so obviously in the experiment because of several factors. First, this averaging process for  $1 < \nu < 2$  tends to obscure the nonparabolicity, which without the averaging would be revealed by two cyclotron-resonance absorptions with different energies, diverging at high field. Second, at low filling factors, the statistics obviously preclude measurements of higher  $n_\nu$  transitions, which would probe the mass further up the band. Finally, the data for ME541 with the lowest carrier concentration, can only be used unambiguously for effective-mass determinations away from the quantum

limit, i.e., at low fields,  $< 7.4$  T, due to localization phenomena. Figure 3 shows how at low field the calculated cyclotron-resonance transitions differ by an amount that is less than the linewidth. It is therefore difficult to compare the low-field mass for samples with different carrier concentrations. Essentially then we can only compare the mass for different carrier concentrations at high field, providing that the quantum limit is not reached. This limits us here to only a small range of carrier concentrations  $3.7\text{--}4.3 \times 10^{11} \text{ cm}^{-2}$ , and we find for each case (ME539 light, ME538 and ME540) that the mass is 0.16 to within 0.005. The complications of cyclotron resonance for the particular series of samples used have thus made it experimentally difficult to reveal the nonparabolicity of the band.

### B. Violation of Kohn's theorem $1 < \nu < 2$

Figure 3 shows also the linewidth (full width at half maximum) of the cyclotron resonance for ME540. For ME540  $\nu = 1$  (2) occurs at  $B = 17.4$  T (8.7 T). At 14 T (17 T) the linewidth is a factor of  $2.2 \pm 0.2$  ( $4.5 \pm 0.7$ ) smaller than the splitting between the two calculated lines, and so it appears that for  $1 < \nu < 2$  the two expected transitions have been hybridized into the single resonance observed experimentally. This result is not dependent on the parameters chosen in the model. For instance, we have calculated the Landau levels for 15%, 18%, and 20% indium, and find that the Landau levels for 18% probably agree best with the cyclotron-resonance data (and 18% also gives the correct quantum-well band gap), but that for all three indium concentrations the  $-2 \rightarrow -1$ ,  $1 \rightarrow 2$  splitting is several times larger than the resonance linewidth. It is difficult to see how an impurity or localizing potential could have this effect. Instead, we suggest that hole-hole interactions are responsible, although the exact nature of the hybridization is unclear. Recent calculations<sup>25</sup> of the magnetoplasmon dispersion for a two-dimensional electron system for  $2 < \nu < 3$  have shown how the two transitions with the same spin can hybridize even in the long-wavelength limit relevant for cyclotron resonance. This explains some recent results of Watts *et al.*,<sup>26</sup> who studied the cyclotron resonance in extremely high-mobility *n*-type GaAs/Al<sub>x</sub>Ga<sub>1-x</sub>As heterostructures and, despite the very narrow linewidth, could not resolve a splitting of the resonance due to nonparabolicity. However, Watts *et al.*<sup>26</sup> also observed only a single resonance when two one-particle transitions of opposite spin were expected. The mixing here is also basically between two transitions of opposite spin,  $M_J = \pm \frac{3}{2}$ , but the spin character of each transition is not so clear cut as in the electron case because of a small admixture of  $M_J = -\frac{1}{2}$  to the predominantly  $M_J = -\frac{3}{2}$ ,  $n_\nu = -1$  level, and admixture of  $M_J = \pm \frac{1}{2}$  to the predominantly  $M_J = +\frac{3}{2}$ ,  $n_\nu = 1, 2$  levels. We therefore propose that the two one-particle cyclotron transitions for  $1 < \nu < 2$  are coupled by many carrier effects, and the complicated makeup of the valence-band spin, in addition to the effects of any disorder in the material, allow the coupling of transitions with basically opposite spin. Kohn's

theorem<sup>27</sup> states that cyclotron resonance is not affected by interactions of the form  $\sum_{i,j} u(\mathbf{r}_i - \mathbf{r}_j)$ . The result only applies for a parabolic system, and it is the nonparabolicity that allows the theorem to be violated in the present case. The nonparabolicity is mainly caused by the  $|M_J| = \frac{3}{2}$  and  $\frac{1}{2}$  mixing. Watts *et al.*<sup>26</sup> required samples with ultrahigh mobilities to study these effects. We can make similar conclusions for holes in this study, albeit from more limited data, with mobilities several orders of magnitude lower, because the spin effects are very much more pronounced in the valence band than in the conduction band. Our results are consistent with recent calculations<sup>28</sup> of the hole magnetoplasmon dispersion for *p*-type GaAs/Al<sub>x</sub>Ga<sub>1-x</sub>As quantum wells, which predict that the  $-2 \rightarrow -1$ ,  $1 \rightarrow 2$  transitions are coupled.

### C. Offset behavior for $\nu < 1$

It was mentioned in Sec. IV A that for  $\nu < 1$ ,  $E_{CR}$  is enhanced. For ME541 in the dark,  $p_s = 1.5 \times 10^{11} \text{ cm}^{-2}$  and  $\nu = 1$  occurs at  $B = 6.2 \text{ T}$ , and almost all the resonances were thus recorded in the quantum limit. Figure 2 shows how the  $E_{CR}$  data points lie above those from samples with higher  $p_s$ . After illumination,  $p_s = 1.8 \times 10^{11} \text{ cm}^{-2}$ , and at low fields  $E_{CR}$  is not enhanced. The transition to an enhanced  $E_{CR}$  takes place around 10 T, which is slightly higher than the fundamental field (7.4 T). Figure 4 shows  $(E_{CR})^2$  plotted against  $B^2$ .  $(E_{CR})^2$  is a linear function of  $B^2$  both in the

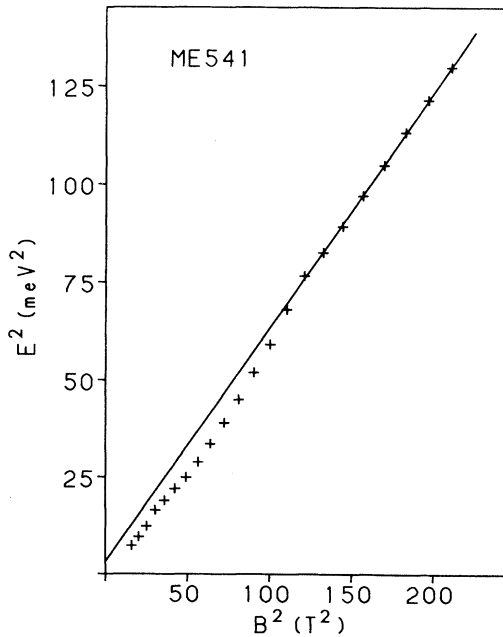


FIG. 4. The cyclotron energy squared plotted against magnetic field squared for ME541 after illumination ( $p_s = 1.8 \times 10^{11} \text{ cm}^{-2}$ ). The line is a straight line fit to the high-field points.

low- and high-field regimes, but the high-field points extrapolate back at  $B^2 = 0$  to  $(E_{CR})^2 = 3.2 \text{ meV}^2$  ( $E_{CR} = 1.8 \pm 0.4 \text{ meV}$ ). ME539 also shows an enhanced  $E_{CR}$  before illumination ( $p_s = 2.6 \times 10^{11} \text{ cm}^{-2}$ ), but a pronounced transition on an  $(E_{CR})^2$  versus  $B^2$  plot was not observed. The enhancement for ME539 disappeared on increasing the carrier concentration to  $p_s = 3.7 \times 10^{11} \text{ cm}^{-2}$  by illumination. The other samples, ME540 and ME538, had higher carrier concentrations (Table I), and so the  $\nu < 1$  range could not be reached experimentally.

These results, particularly those for ME541, suggest that the cyclotron resonance is influenced by disorder potentials in the samples. This  $(E_{CR})^2$  versus  $B^2$  behavior has been observed in two-dimensional (2D) *n*-type systems,<sup>29-32</sup> and Sigg, Weiss, and Klitzing<sup>29</sup> showed how the offset is dependent on the degree of disorder, controlled in this case by high-energy electron bombardment. The main difference is that the enhanced  $E_{CR}$  was observed for  $\nu < 2$  in the *n*-type systems, whereas it is observed here for  $\nu < 1$ . This is simply a consequence of the different spin splittings, which are very small in the GaAs conduction band but are important in the valence band, so that the quantum limit is reached essentially at  $\nu = 2$  for GaAs 2D electrons but not until  $\nu = 1$  for the 2D holes. A simple explanation of the effect assumes that the potential fluctuations vary over a distance that is large compared to the cyclotron radius  $l_c$  at high field ( $l_c = \sqrt{\hbar/eB}$ ). In the quantum limit, all the carriers reside only in the lowest Landau level, and within that level they fill the states with lowest energy, and so as the field is increased the carriers become localized in the potential fluctuations. The bottom of the potential fluctuations may have an approximately parabolic form. For a one-dimensional wire extending in, say, the *y* direction with parabolic walls,  $\frac{1}{2}m^*\delta^2x^2$ , the cyclotron-resonance energy  $E_{CR}$  for a field along *z* is given by<sup>33</sup>

$$(E_{CR})^2 = (E_{CR}^0)^2 + (\hbar\delta)^2, \quad (1)$$

where  $E_{CR}^0 = e\hbar B/m^*$ , the cyclotron energy without the additional parabolic potential. A similar result is found for deliberately patterned “quantum-dot” structures.<sup>34</sup> In the quantum limit, then, we propose that all the holes are bound in approximately parabolic potential fluctuations, so that the  $(\hbar\delta)^2$  term explains the enhancement of  $E_{CR}$  compared to  $E_{CR}^0$ . We note that Kohn’s theorem still applies with the additional parabolic potential in this geometry,<sup>35</sup> and so if one ignores the nonparabolicity in the electronic band structure, the parabolic potential fluctuation is the bare unscreened potential. In fact, Kohn’s theorem generally applies when there are parabolic potentials,<sup>36</sup> and so carrier-carrier interactions have little effect on the far-infrared response of quantum dots<sup>34,36,37</sup> that have approximately parabolic confinement potentials. The localizing potential in 2D systems arises from both well fluctuations and impurities, and also in this case alloy disorder is likely to be important as the quantum well material is the  $\text{In}_{0.18}\text{Ga}_{0.82}\text{As}$ . Once the first Landau level is completely full, the transitions from this level no longer follow the offset behavior as the potential fluctua-

tions tend to be averaged out. The higher Landau levels will be less influenced by the potential fluctuations than the first if the  $E_{\text{CR}}^0$  energies are comparable to or larger than the heights of the potential fluctuations. This must be the case experimentally, because an enhanced  $E_{\text{CR}}$  is only observed in the quantum limit. It is difficult to estimate the properties of the potential fluctuations from these results, as the effect depends most on the filling factor. However, the numbers are at least consistent with a picture based on the localization of the carriers into potential fluctuations. At 10 T,  $E_{\text{CR}}^0 \approx 7.2$  meV and  $l_c \approx 81$  Å, and when the potential  $\frac{1}{2}m^* \delta^2 x^2 = E_{\text{CR}}^0$  we find  $x = 460$  Å for  $\hbar\delta = 1.8$  meV (ME541), which is indeed larger than  $l_c$ . It would appear that the potential fluctuations are a few meV deep and extend over a few hundred Å.

#### D. Linewidth measurements

Figure 5 shows the cyclotron linewidths and effective masses for samples ME540, ME538, and ME539. For ME540 ( $p_s = 4.2 \times 10^{11} \text{ cm}^{-2}$ ) the linewidth varies between  $0.7 \pm 0.1$  and  $1.4 \pm 0.1$  meV, reaching a maximum at  $\nu \approx 1.5 \pm 0.1$ . ME538 ( $p_s = 3.7$  and  $4.0 \times 10^{11} \text{ cm}^{-2}$ ) behaved similarly, having a linewidth maximum at  $\nu \approx 1.4$ . In addition, at lower field the linewidth peaks at a filling factor somewhere between  $\nu = 2$  and 3, with a maximum linewidth that is about the same as the

linewidth maximum at the  $\nu \approx 1.4$  anomaly. For ME539, after illumination ( $p_s = 3.7 \times 10^{11} \text{ cm}^{-2}$ ) the linewidth peaked at  $\nu \approx 1.3$ . Precise linewidth measurements at lower  $p_s$  were rather difficult because of the weak absorption. There is then a maximum linewidth that appears to be tied to a filling factor of  $\nu \approx 1.4$ . Again, similar linewidth fluctuations have been seen in the cyclotron resonance of *n*-type systems,<sup>31,38-40</sup> and again we can make an analogy between  $\nu = 2$  in the *n*-type case when the spin splitting is not important and  $\nu = 1$  here, where the spin splitting is important. The experimental situation can be rather complex, however.<sup>40</sup>

A modified Kramers-Kronig analysis was used by Nicholas *et al.*<sup>31</sup> to relate the linewidth and mass anomalies. The appearance of an offset in the cyclotron resonance energy at  $\nu = 2$  determines and is determined by a linewidth anomaly at a similar filling factor. However, in these experiments it was not possible to simultaneously measure the linewidth accurately and observe the offset because we could not reach the quantum limit for the high-density samples, and we could not accurately measure the linewidth for the low-density sample ME541 due to the rather weak absorption ( $\sim 2\%$ ). Figure 5 shows how the  $\nu \approx 1.4$  linewidth peak does not correspond with any obvious anomaly in the mass. It could be that the  $\nu \approx 1.4$  anomaly is related to a quantum limit offset behavior in the cyclotron energy but is shifted down in field.

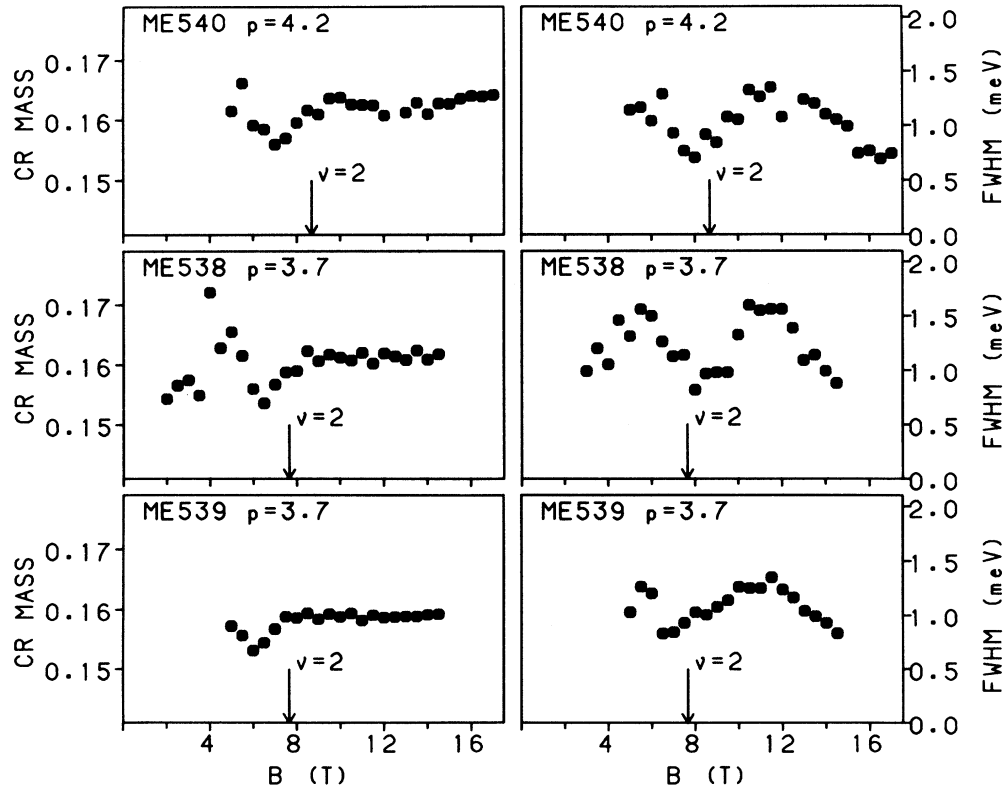


FIG. 5. The cyclotron mass (in units of the free-electron mass) and cyclotron-resonance FWHM plotted against magnetic field for ME540 ( $p_s = 4.2 \times 10^{11} \text{ cm}^{-2}$ ), ME538 ( $p_s = 3.7 \times 10^{11} \text{ cm}^{-2}$ ), and ME539 ( $p_s = 3.7 \times 10^{11} \text{ cm}^{-2}$ ).

A further effect should be considered. The screening by the carriers of the ionized impurity potential is strongly filling-factor dependent. When the Fermi energy lies between two Landau levels, the screening is suppressed, causing the resonance to broaden. This has been calculated<sup>41</sup> and observed<sup>38,39</sup> exactly at even filling factors. The existing calculations<sup>41</sup> assume that remote ionized impurity scattering is dominant, and it is not clear how to apply the results to the case here, when it has already been shown that carrier-carrier interactions and localizing potentials are important. Also, the theory predicts that the cyclotron resonance is broadened but not shifted in energy by the impurity potentials. We find in these results that shifts in the cyclotron energy do occur. Although the linewidth maximum at  $\nu \approx 1.4$  has no obvious correspondence with the mass, which is almost constant in this field range (Fig. 5), the linewidth anomaly at lower field (ME538) does coincide with structure in the mass-versus-field plot, in which the mass changes by  $\pm 0.01$ . We suggest, therefore, that oscillatory screening is likely to be important, but that it must be considered along with the other interactions that perturb the cyclotron resonance to explain these results.

We have shown that the 2D hole cyclotron resonance is affected by carrier-carrier interactions and by localizing potentials. Similar results have been observed in *n*-type systems, including studies of ultrahigh mobility GaAs/Al<sub>x</sub>Ga<sub>1-x</sub>As heterostructures.<sup>26,31,40</sup> It would appear then that these effects, which go beyond an intrinsic one-particle picture of cyclotron resonance and complicate an attempt at effective-mass determination, may be general features of cyclotron resonance in two dimensions. We comment also that the strain makes the hole mass light and the valence-band Landau levels relatively simple, and these effects have enabled us to study in detail cyclotron resonance of 2D holes.

## V. INTERBAND MAGNETO-OPTICS

Figure 6 shows some photoconductivity spectra at 4 K and at several magnetic fields for sample ME540 ( $p_s = 4.3 \times 10^{11} \text{ cm}^{-2}$ ). The zero-field trace consists essentially of a broad onset of photoconduction, which we expect to occur at the band gap plus Fermi energy. This is indeed likely to be the case, as the high-field points extrapolate back at  $B = 0$  to an energy where the photoresponse is just beginning. No excitonlike features could be seen at zero field. On applying a magnetic field, sharp Landau-level transitions emerge. Figure 7 is a fan diagram, a plot of the transition energies versus magnetic field. Also plotted are the results for ME541 ( $p_s = 1.8 \times 10^{11} \text{ cm}^{-2}$ ). We observed that the strength of the photoconductivity signal was very field dependent. Indeed, we plotted the response at  $\approx 1.4 \text{ eV}$  as a function of magnetic field and found that the trace was similar to the Shubnikov-de Haas oscillations of the magnetoresistance. The photoconductivity essentially disappears when the Fermi energy lies between two Landau levels and the conductivity is small. This is experimentally inconvenient, as it makes it difficult to measure interband spectra over the entire field range. The fan diagrams for

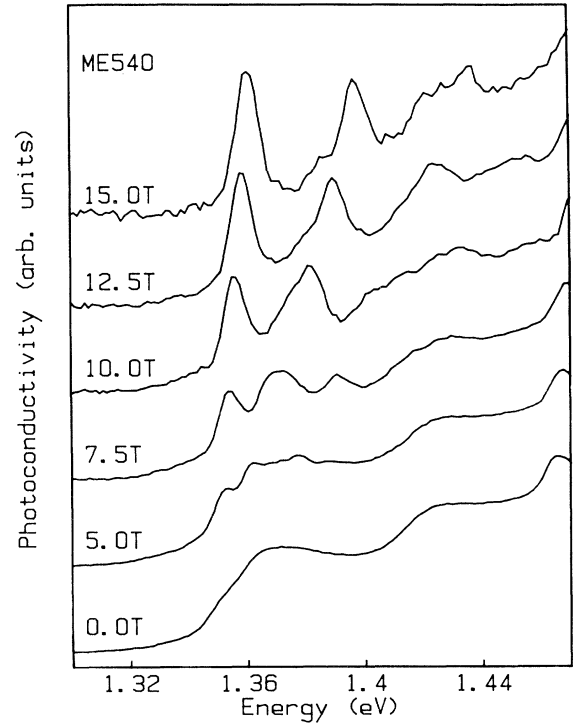


FIG. 6. Photoconductivity spectra for sample ME540 at several magnetic fields.

ME540 and ME541 are similar, except that the ME541 band gap is about  $\approx 10 \text{ meV}$  higher, which could be easily explained by a slight difference in either indium concentration or well width between the two samples.

To calculate the interband energies from the Landau levels, we have derived the selection rules for transitions between the valence and conduction bands, and we have then modeled the magnetoexciton binding energy. The selection rules are

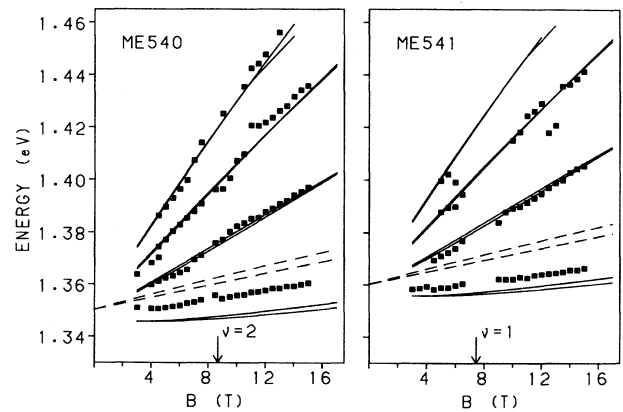


FIG. 7. Fan diagrams for samples ME540 ( $p_s = 4.3 \times 10^{11} \text{ cm}^{-2}$ ) and ME541 ( $p_s = 1.8 \times 10^{11} \text{ cm}^{-2}$ ). The solid lines are the calculated magnetoexciton energies taking a zero-field exciton binding energy  $E_{ex}(0) = 8 \text{ meV}$ . The dashed lines are the free-electron transitions, calculated for  $E_{ex}(0) = 0$  and  $n_l = 0$ .

$$n_v \rightarrow n_v + 1 \quad \text{for } M_J = -\frac{3}{2}, \quad n_v = -2, -1, 0, \dots, \quad (2)$$

$$n_v \rightarrow n_v - 1 \quad \text{for } M_J = +\frac{3}{2}, \quad n_v = 1, 2, 3, \dots, \quad (3)$$

which correspond to transitions with opposite circular polarization. A spin splitting was not resolved experimentally, and so it would appear that each transition is made up of two components. The interband spin splitting is dominated by the valence-band spin splitting, as the conduction-band spin splitting is rather small in this material system. The linewidth of the interband transition at high field is larger than any calculated valence spin splitting, and this tells us that the value of  $\kappa_l$ , the Luttinger parameter,<sup>23</sup> deduced from our transport experiments,<sup>42</sup> is not overestimated. No other transitions were obvious in the spectra in the energy range of Fig. 7. This confirms that the selection rules, derived by assuming decoupled valence bands, are adequate, and are another example of the simplification brought about by the strain. Exciton effects are known to be important in undoped  $\text{In}_x\text{Ga}_{1-x}\text{As}/\text{GaAs}$  quantum wells. To account for the exciton effect, and to discuss the additional effects caused by the doping in these structures, we assume we know the zero-field exciton binding energy  $E_{\text{ex}}(0)$  of an undoped 90-Å  $\text{In}_{0.18}\text{Ga}_{0.82}\text{As}/\text{GaAs}$  quantum well. We can do this from the work of Moore *et al.*,<sup>43</sup> who calculated the exciton binding energy as a function of well width for  $\text{In}_{0.15}\text{Ga}_{0.85}\text{As}/\text{GaAs}$  quantum wells, and achieved good agreement with their experimental results. For a 90-Å  $\text{In}_{0.15}\text{Ga}_{0.85}\text{As}/\text{GaAs}$  quantum well, Moore *et al.*<sup>43</sup> calculate  $E_{\text{ex}}(0) = 8$  meV. We have taken  $E_{\text{ex}}(0) = 8$  meV in the subsequent analysis, ignoring the 3% difference in indium concentration between our own quantum wells and the calculations of Moore *et al.* We have used a semi-empirical model for the magnetoexciton,<sup>22</sup> an adaptation of the Akimoto-Hasegawa<sup>44</sup> high-field result for nonparabolic bands. We expect that interband transitions from hole levels well above the Fermi energy will not be strongly influenced by the presence of the carriers. For these transitions we can confidently model the data with the theory as for undoped quantum wells. In any case, Akimoto and Hasegawa<sup>44</sup> derive that the magnetoexciton binding energy is proportional to  $(n_l + \frac{1}{2})^{-1/2}$ , where  $n_l$  is the conventional index of the interband transitions. ( $n_v = -2 \rightarrow -1$  and  $n_v = 1 \rightarrow 0$  comprise  $n_l = 0$ , etc.) The influence of the magnetoexciton binding thus reduces with increasing  $n_l$ .

To fit the data for ME540, the parameters of Table II and  $E_{\text{ex}}(0) = 8$  meV were used. For ME541, the calculations were rigidly shifted by 10 meV to fit the  $n_l = 1, 2$ , and 3 levels. The solid lines in Fig. 7 show the magnetoexciton energies calculated with the above selection rules and the magnetoexciton model. The theory gives a good fit to the experimental points except for the  $n_l = 0$  transition. Essentially, the interband experiment measures the conduction mass and nonparabolicity if we assume we know the valence-band Landau levels from the cyclotron resonance.

In Fig. 7 we plot also the  $n_l = 0$  energies for  $E_{\text{ex}}(0) = 0$  (dashed lines). These are the free-electron transition energies, without any exciton binding. The data for ME540

lie roughly midway between the solid and dashed lines, but for ME541 the data lie nearer to the solid lines. The difference between the dashed lines and the experimental points measures the magnetoexciton binding energy. Assuming that  $E_{\text{ex}}(0) = 8$  meV is accurate, we can deduce that the exciton binding energy is reduced by the presence of the holes, and that this effect is more pronounced at a particular field for the more heavily doped sample ME540 than for ME541. The exciton has been observed to quench in *n*-type systems, attributed to phase-space filling, and screening effects.<sup>45,46</sup> Recently, in a GaAs *n*-type quantum well, a transition from free-carrier recombination to excitonic recombination<sup>47</sup> has been deduced on increasing the magnetic field (in a photoluminescence experiment). We expect that the excitonic fits in Fig. 7 (solid lines) will be good once the lowest Landau level is only sparsely occupied by holes, i.e., in the quantum limit, at very high fields. For ME541 the quantum limit is reached at  $B = 7.4$  T. The excitonic fit is much better than the free-carrier fit for this sample (Fig. 7). This qualitatively corresponds with the *n*-type results, as it suggests that the quenching of the binding energy is less severe at lower carrier concentrations, or, equivalently, at lower filling factors.

The strengths of the different transitions show an unusual behavior in that the first interband Landau level could be observed for fields greater than about 4 T for both ME540 and ME541. The  $-2 \rightarrow -1$  ( $1 \rightarrow 0$ ) transition should only be observed when the  $-2$  ( $1$ ) level begins to empty of holes, i.e., for  $\nu < 1$  ( $\nu < 2$ ). So at  $T = 0$  and for unbroadened Landau levels the first interband Landau level should not be observed at all until  $\nu < 2$ , which corresponds to  $B > 8.9$  T ( $B > 3.7$  T) for ME540 (ME541). We could observe the first transition for  $B \geq 4$  T, i.e.,  $\nu > 2$ , for ME540. Figure 6 shows spectra at 5.0 and 7.5 T, both below the  $\nu = 2$  field, and considerably below the  $\nu = 1$  field. It is unlikely that thermal broadening is significant at these temperatures. At  $B = 4$  T the spacing of, say, the  $n_v = 1$  and  $-1$  levels (see Fig. 1) is  $\sim 6$  times larger than  $kT$  at 4.2 K and so occupation of the  $n_v = 1$  level with electrons will be very small at this field and insufficient to account for the intensity of the first interband transition. The Landau levels will be broadened, of course, by defects, but this too cannot account for the observation of the first interband transition at  $\nu > 2$ . A large broadening would be required to spread the occupation of holes over several Landau levels, and this would not be compatible with the well-resolved cyclotron-resonance and magnetotransport data. Our results are actually similar to those reported by Iwasa, Lee, and Miura<sup>48</sup> and Lee, Miura and Iwasa<sup>49</sup> on *p*-type GaAs/ $\text{Al}_x\text{Ga}_{1-x}\text{As}$  quantum wells. These authors measured transmission as a function of field and observed a sharp increase in the intensity of the “heavy-hole exciton” at a particular field  $B_{\text{th}}$ .  $B_{\text{th}}$  increases with  $p_s$ , but is much smaller than the quantum limit field. Their interpretation takes a one-particle view of the effects of band filling. They claim that because the lowest exciton wave function is formed from a superposition of Landau levels, the lowest-energy transition can be observed as the higher levels depopulate. Optical experiments on *n*-type



samples have not revealed any similar effects,<sup>50</sup> and, in fact, the results were used to probe the movement of the Fermi energy in the conduction band. The difference between the  $n$ - and  $p$ -type cases may be caused by the different masses of the two bands. The hole is heavier than the electron and is thus more localized within the exciton than the electron.

Valence-band Landau-level mixing is expected to be unimportant only at high field when the cyclotron radius  $l_c$  is less than the spatial extent of the hole. We attempt to quantify this argument with a semiclassical analysis. Taking a Fourier transform of the exciton wave function in a simple hydrogenic model at zero field, we estimate the spread in  $\mathbf{k}$  space of the hole  $\delta k_h$  by taking the half-width of the resulting Lorentzian. We then compare  $1/\delta k_h$  to the cyclotron radius  $l_c$ . This defines a magnetic field when valence-band mixing in the exciton wave function has become unimportant. We find that this limit is 16 T for a 3D exciton, and 64 T for a 2D exciton in our samples. These limits scale as the square of the effective mass and so are very much lower for the conduction band in  $n$ -type samples. The real exciton in our samples is somewhere between the two- and three-dimensional ideals. In either case, valence-band mixing in the exciton wave function is likely to be important for ME540, where the field for  $\nu=2$  is at 8.9 T. The  $n_l=0$  transition is then allowed at low field through the admixture of unoccupied states to the exciton wave function.

Finally, we comment that the light mass in this system makes it easy to produce samples in which the Fermi energy  $E_F$  is much greater than  $kT$ . By comparison, the heavy-hole mass is typically very large in wide unstrained  $p$ -type quantum wells, giving smaller Fermi energies as, of course,  $E_F \propto m^{-1}$ . For instance, Iwasa, Lee, and Miura<sup>48</sup> used samples in which  $E_F \approx kT$ . In principle, strained-layer samples with  $E_F \gg kT$  could be ideal to

study the influence of many-body effects on the optical properties of two-dimensional holes.

## VI. CONCLUSIONS

We report an investigation of a series of  $p$ -type  $\text{In}_{0.18}\text{Ga}_{0.82}\text{As}/\text{GaAs}$  quantum wells. The important point is that the uniaxial component of the strain splits the “heavy-hole”  $|M_J|=\frac{3}{2}$  and “light-hole”  $|M_J|=\frac{1}{2}$  states. We show how this results in a light in-plane mass for the first  $|M_J|=\frac{3}{2}$  subband and a simple set of interband selection rules. Both cyclotron-resonance and interband photoconductivity experiments are modeled with an eight-band  $\mathbf{k}\cdot\mathbf{p}$  calculation of the Landau levels interpreted in a one-particle framework. Good agreement with experiment is obtained. Evidence is presented for the hybridization of the two-cyclotron-resonance transitions for  $1 < \nu < 2$ , and this is compatible with recent theoretical ideas about hole magnetoplasmons.<sup>28</sup> Residual mixing of the  $|M_J|=\frac{3}{2}$  and  $\frac{1}{2}$  states causes the subbands to be non-parabolic, and hence Kohn’s theorem<sup>27</sup> does not apply. The cyclotron-resonance energy is enhanced for  $\nu < 1$ , and this is interpreted as a quantization of the holes into localizing potentials. The linewidth and cyclotron mass have anomalies at higher filling factors, which suggests that a complete interpretation of the cyclotron resonance data would be very involved. In all these respects, the cyclotron resonance behaves similarly to  $n$ -type systems, but with some quantum-limit effects shifted to  $\nu \approx 1$  due to the much larger effective spin splitting in the valence band. This leads us to suggest that these effects are general to cyclotron resonance in two dimensions. The  $n_l=0$  interband transition is shown to have a reduced magnetoexciton binding energy in these  $p$ -doped structures, and, surprisingly, the  $n_l=0$  interband transition could be observed at fields well below the quantum-limit field.

<sup>1</sup>E. P. O’Reilly and G. P. Witchlow, *Solid State Commun.* **62**, 653 (1987).

<sup>2</sup>J. E. Schirber, I. J. Fritz, and L. R. Dawson, *Appl. Phys. Lett.* **46**, 187 (1985).

<sup>3</sup>S. Y. Lin, C. T. Liu, D. C. Tsui, E. D. Jones, and L. R. Dawson, *Appl. Phys. Lett.* **55**, 666 (1989).

<sup>4</sup>D. Lancefield, W. Batty, C. G. Crookes, E. P. O’Reilly, A. R. Adams, K. P. Homewood, G. Sundaram, R. J. Nicholas, M. Emeny, and C. R. Whitehouse, *Surf. Sci.* **229**, 122 (1990).

<sup>5</sup>G. C. Osbourn, J. E. Schirber, T. J. Drummond, L. R. Dawson, B. L. Doyle, and I. J. Fritz, *Appl. Phys. Lett.* **49**, 731 (1986).

<sup>6</sup>E. D. Jones, R. M. Biefeld, J. F. Klem, S. K. Lyo, and G. C. Osbourn, *Surf. Sci.* **228**, 330 (1990).

<sup>7</sup>E. P. O’Reilly, *Semicond. Sci. Technol.* **4**, 121 (1989).

<sup>8</sup>A. Fasolino and M. Altarelli, in *Two Dimensional Systems, Heterostructures and Superlattices*, edited by G. Bauer, F. Kuchar, and H. Heinrich (Springer-Verlag, Berlin, 1984), Vol. 53, p. 176.

<sup>9</sup>T. Ando, *J. Phys. Soc. Jpn.* **54**, 1528 (1985).

<sup>10</sup>H. L. Stormer, Z. Schlesinger, A. Chang, D. C. Tsui, A. C. Gossard, and W. Wiegmann, *Phys. Rev. Lett.* **51**, 126 (1983).

<sup>11</sup>E. E. Mendez, *Surf. Sci.* **170**, 561 (1986).

<sup>12</sup>J.-Y. Marzin, M. N. Charasse, and B. Sermage, *Phys. Rev. B* **31**, 8298 (1985).

<sup>13</sup>D. Gershoni, J. M. Vandenberg, S. N. G. Chu, H. Temkin, T. Tanbun-Ek, and R. A. Logan, *Phys. Rev. B* **40**, 10017 (1989).

<sup>14</sup>G. Duggan, K. J. Moore, K. Woodbridge, C. Roberts, N. J. Pulsford, and R. J. Nicholas, in *Semiconductor Optical Properties*, edited by J. L. Beeby (Plenum, New York, 1991), p. 509.

<sup>15</sup>N. J. Pulsford, R. J. Nicholas, R. J. Warburton, G. Duggan, K. J. Moore, K. Woodbridge, and C. Roberts, *Phys. Rev. B* **43**, 2246 (1991).

<sup>16</sup>W. H. Weiler, in *Semiconductors and Semimetals*, edited by R. K. Willardson and A. C. Beer (Academic, New York, 1981), Vol. 16, p. 119.

<sup>17</sup>R. Eppenga, M. F. H. Schuurmans, and S. Colak, *Phys. Rev. B* **36**, 1554 (1987).

<sup>18</sup>G. E. Pikus and G. L. Bir, *Fiz. Tverd. Tela (Leningrad)* **1**, 1642 (1959) [*Sov. Phys.—Solid State* **1**, 1502 (1960)].

<sup>19</sup>B. V. Shanabrook, O. J. Glembocki, D. A. Broido, and W. I. Wang, *Superlatt. Microstruct.* **5**, 503 (1989).

- <sup>20</sup>J.-P. Reithmaier, R. Höger, H. Riechert, A. Herberle, G. Abstreiter, and G. Weimann, *Appl. Phys. Lett.* **56**, 536 (1990).
- <sup>21</sup>L. R. Ram-Mohan, K. H. Yoo, and R. L. Aggarwal, *Phys. Rev. B* **38**, 6151 (1988).
- <sup>22</sup>R. J. Warburton, G. M. Sundaram, R. J. Nicholas, S. K. Haywood, G. J. Rees, N. J. Mason, and P. J. Walker, *Surf. Sci.* **228**, 270 (1990).
- <sup>23</sup>J. M. Luttinger, *Phys. Rev.* **102**, 1030 (1956).
- <sup>24</sup>F. Thiele, U. Merkt, J. P. Kotthaus, G. Lommer, F. Malcher, U. Rössler, and G. Weimann, *Solid State Commun.* **62**, 841 (1987).
- <sup>25</sup>A. H. MacDonald and C. Kallin, *Phys. Rev. B* **40**, 5795 (1989).
- <sup>26</sup>M. Watts, R. J. Nicholas, N. J. Pulsford, J. J. Harris, and C. T. Foxon, in *Proceedings of the 20th International Conference on the Physics of Semiconductors, Thessaloniki*, edited by E. M. Anastassakis and J. D. Joannopoulos (World Scientific, Singapore, 1990), Vol. 2, p. 1465.
- <sup>27</sup>W. Kohn, *Phys. Rev.* **123**, 1242 (1961).
- <sup>28</sup>S.-R. Eric Yang and A. H. MacDonald, *Phys. Rev. B* **41**, 1294 (1990).
- <sup>29</sup>H. Sigg, D. Weiss, and K. v. Klitzing, *Surf. Sci.* **196**, 293 (1988).
- <sup>30</sup>J. Richter, H. Sigg, K. v. Klitzing, and K. Ploog, *Phys. Rev. B* **39**, 6268 (1989).
- <sup>31</sup>R. J. Nicholas, M. A. Hopkins, D. J. Barnes, M. A. Brummell, H. Sigg, D. Heitmann, K. Ensslin, J. J. Harris, C. T. Foxon, and G. Weimann, *Phys. Rev. B* **39**, 10955 (1989).
- <sup>32</sup>G. Wiggins, R. J. Nicholas, J. J. Harris, and C. T. Foxon, *Surf. Sci.* **229**, 488 (1990).
- <sup>33</sup>J. P. Kotthaus, G. Abstreiter, J. F. Koch, and R. Ranvaud, *Phys. Rev. Lett.* **34**, 151 (1975).
- <sup>34</sup>Ch. Sikorski and U. Merkt, *Phys. Rev. Lett.* **62**, 2164 (1989).
- <sup>35</sup>L. Brey, N. F. Johnson, and B. I. Halperin, *Phys. Rev. B* **40**, 10647 (1989).
- <sup>36</sup>F. M. Peeters, *Phys. Rev. B* **42**, 1486 (1990).
- <sup>37</sup>P. A. Maksym and Tapash Chakraborty, *Phys. Rev. Lett.* **65**, 108 (1990).
- <sup>38</sup>Th. Englert, J. C. Maan, Ch. Uihlein, D. C. Tsui, and A. C. Gossard, *Solid State Commun.* **46**, 545 (1983).
- <sup>39</sup>D. Heitmann, M. Ziesmann, and L. L. Chang, *Phys. Rev. B* **34**, 7463 (1986).
- <sup>40</sup>K. Ensslin, D. Heitmann, H. Sigg, and K. Ploog, *Phys. Rev. B* **36**, 8177 (1987).
- <sup>41</sup>T. Ando and Y. Murayama, *J. Phys. Soc. Jpn.* **54**, 1519 (1985).
- <sup>42</sup>R. J. Warburton, R. W. Martin, R. J. Nicholas, L. K. Howard, and M. T. Emeny, *Semicond. Sci. Technol.* (to be published).
- <sup>43</sup>K. J. Moore, G. Duggan, K. Woodbridge, and C. Roberts, *Phys. Rev. B* **41**, 1090 (1990).
- <sup>44</sup>H. Akimoto and H. Hasegawa, *J. Phys. Soc. Jpn.* **22**, 181 (1967).
- <sup>45</sup>C. Delalande, G. Bastard, J. Orgonasi, J. A. Brum, H. W. Liu, M. Voos, G. Weimann, and W. Schlapp, *Phys. Rev. Lett.* **59**, 2690 (1987).
- <sup>46</sup>H. Yoshimura, G. E. W. Bauer, and H. Sakaki, *Phys. Rev. B* **38**, 10791 (1988).
- <sup>47</sup>H. Yoshimura and H. Sakaki, *Surf. Sci.* **229**, 508 (1990).
- <sup>48</sup>Y. Iwasa, J. S. Lee, and N. Miura, *Solid State Commun.* **64**, 597 (1987).
- <sup>49</sup>J. S. Lee, N. Miura, and Y. Iwasa, *Solid State Commun.* **69**, 293 (1989).
- <sup>50</sup>B. B. Goldberg, D. Heiman, M. J. Graf, D. A. Broido, A. Pinczuk, C. W. Tu, J. H. English, and A. C. Gossard, *Phys. Rev. B* **38**, 10131 (1988).